

# PROTOTYPING MILLIROBOTS USING DEXTRIOUS MICROASSEMBLY AND FOLDING \*

E. Shimada, J.A. Thompson, J. Yan, R. Wood and R.S. Fearing<sup>†</sup>

Department of Electrical Engineering and Computer Science

University of California

Berkeley, CA 94720-1770

## ABSTRACT

This paper discusses two processes for rapidly prototyping micromechanical systems: first microassembly, and second, laser cutting of thin sheets and folding. Sub-millimeter rigid blocks can be dextrously manipulated using two 1 DOF fingers and an XYZ micro-positioning stage. Algorithms for micro-part manipulation use open-loop compliant grasps combined with slip to align microparts, which can then be adhesively bonded. Strong, lightweight structures with low friction flexural joints can be readily laser cut, then folded. Potentially, thermally driven actuators can be simply integrated with flexural structures to build fingers for part manipulation.

## INTRODUCTION

Microassembly provides the capability to construct 3 dimensional heterogenous microsystems by joining sensors, actuators, structures, and intelligence which are separately fabricated, and ideally available off the shelf. This paper examines applying techniques from conventional-size robotic part manipulation to manipulating sub-millimeter parts. Strategies and simple fixtures which are inherently robust without sensing can be used to manipulate micro-parts.

The problem of robotic microassembly has been explored using high precision actuators and vision feedback in work by Codourey et al [1995], Feddema and Simon [1998], Kasaya et al [1998], Nelson et al [1998], and Sulzmann et al [1998]. Vision-based approaches are limited by poor depth of field of high power microscopes, cluttered views, and lack determination of contact or contact forces. In addition, it is difficult to perform several distinct operations in parallel as microscopes are quite bulky and expensive (although parallel operations can be performed with rigid pallets and fixtures [Feddema and Christensen 1999]). Alternatively, force sensor based approaches can be local and provide exact information about contact between surfaces (Zesch and Fearing [1998], Sitti and Hashimoto [1999], Zhou and Nelson [1998]).

At the micro-scale, adhesion forces of surface tension, elec-

trostatic and Van der Waals dominate gravitational forces (Arai et al [1995], Fearing [1995]). Recent work has shown how adhesive forces can be used to advantage during microassembly tasks by controlling contact areas and surface tension, to ensure that microparts are reliably transferred to the target surface and released from the gripper (Arai and Fukuda [1997], Miyazaki and Sato [1997], Saito et al [1999], Zhou and Nelson [1998], Zesch et al [1997]).

Previous micromanipulation work has used single probes or parallel jaw grippers to manipulate parts. The parallel jaw gripper approach follows from macro-robotics where a simple gripper is used with a 6 degree-of-freedom (DOF) arm to reorient and position parts. As sub-centimeter 6 DOF micro-robot arms are not yet available, we show how macro-scale dextrous manipulation techniques can be used with much simpler mechanisms to reorient and position parts. By using gripping forces which exceed adhesion forces, we can use Coulomb friction to control part sticking and sliding. In this paper, we demonstrate how micro-parts can be dextrously manipulated in open-loop fashion using two 1 DOF fingers in the plane combined with an XYZ cartesian stage.

As shown by [Fearing 1986a] and [Gopalswamy and Fearing 1989] two-finger grasps of polygons and polyhedra (respectively) will automatically slide to a stable configuration if the angle between the included faces is less than twice the friction angle. Conversely, a tangential force at one finger will cause the grasped part to roll about the opposite finger. Alternatively, rotational torques can be applied by a third finger [Fearing 1986a]. As these grasping methods do not require feedback, and are robust to initial conditions, they are well suited to the micro-domain and parallelization. Grasping methods and automatic planners using slip have been discussed further by Brost [1986], Carlisle et al [1994], Erdmann et al [1993], Goldberg [1993], Lynch [1999], Rus [1993], Rao et al [1996], Yoshikawa et al [1993], and Wiegley et al [1997].

Another method of obtaining 3D microstructures is by planar fabrication of polysilicon plates and then folding out of the plane such as Pister et al [1992], using pin hinges, and Shimoyama et al [1993], using polyimide hinges. Microrobot struc-

\*This work was funded in part by NEC, ONR MURI N00014-98-1-0671, ONR DURIP and DARPA. †Corresponding author.

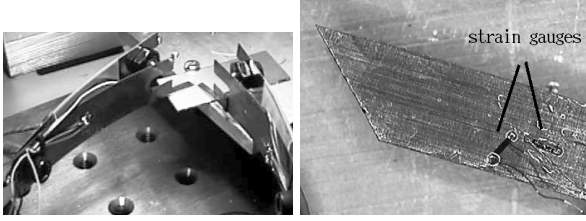


**Figure 1:** a) Perpendicular tweezer tips driven by large piezo beams. b) 1 mm semiconductor strain gauges mounted on stainless steel tweezer tip.

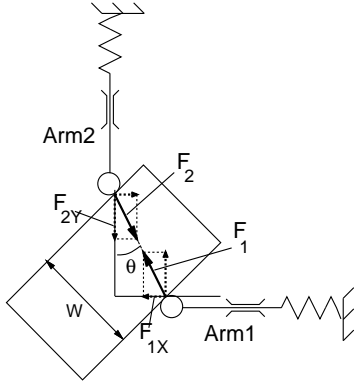


**Figure 2:** Grasping configuration for microparts.

tures have been built using this technology by Yeh et al [1994], although assembly is still by hand. Alternatively, clever interconnection of structures allows complicated structures to be assembled by a single actuator [Hui et al 2000]. Recent work by Lu and Akella [1999] opens the possibility that folding processes can be readily automated using simple fixtures. In this paper, we show how the thorax of a micro-robotic fly can be folded from laser-cut stainless steel. The advantage of stainless steel over polysilicon is the ease of plastic deformation at room temperature to desired shapes, its inherent low cost (pennies per sq. cm.), and ease of processing.

### MICRO-COMPONENT DEXTRIOUS ASSEMBLY

In order to assemble micro-components, we made prototype tweezers for micro-manipulation. Each arm of the tweezers consists of a Thunder TH8-R (<http://www.face-int.com/thunder/>) piezoelectric actuator ( $64 \times 12.7 \times 0.5 \text{ mm}$ ), a base stainless sheet and a tip stainless sheet (Figure 1a). The base stainless sheet is  $0.18 \text{ mm} \times 63 \text{ mm} \times 13 \text{ mm}$ , the tip sheet is  $0.05 \text{ mm} \times 6 \text{ mm} \times 2 \text{ mm}$ , and the tip compliance is  $100 \text{ N/m}$ . The tip sheet is attached to the base sheet. The piezoelectric actuator and base sheet are clamped together at the base, and the base sheet is driven with a point contact at the distal end of the piezo beam. A pair of strain gauges is attached to the base sheet to measure its deflection. Another pair of strain gauges measures the deflection and force at the tip (Figure 1b). Strain gauges ( $1 \text{ mm length} \times 0.15 \text{ mm width}$ ) are Entran ESB-020-350 (<http://www.entran.com>).

The tweezers are fixed in space above the work platform which is mounted on an  $XYZ$  stepping motor stage. We man-

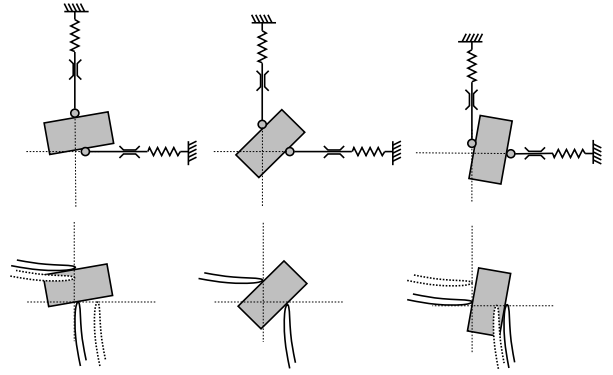


**Figure 3:** In-plane part rolling geometry.

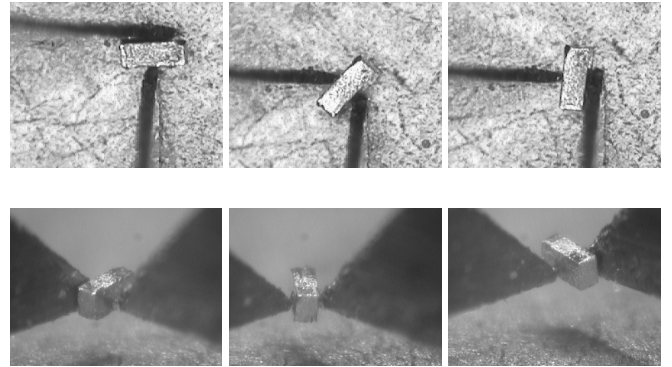


**Figure 4:** Micropart rolling, top and side view.

ually place a micro-component on the substrate and move the substrate stage so that the tweezers can manipulate the component. We arrange the tweezers perpendicular to each other, as shown in Figure 2. (Note that this finger stiffness matrix is the same as for the 1 DOF finger used in [Fearing 1986b]. As shown in that paper, this stiffness matrix guarantees stable grasps, without feedback, for polygons with the included angle between grasp faces less than twice the friction angle.) The perpendicular configuration makes it possible to rotate a micro-component by controlling the deflection of each tweezer arm separately. We define the tip positions of Arm1 and Arm2 as  $(x_1, 0)$  and  $(0, y_2)$ , and assume a point contact. We also define the width and orientation of the micro-component as  $W$  and  $\theta$ . When the tweezers grip the midpoints of opposite sides of the square component,  $x_1 = W \sin(\theta)$  and  $y_2 = W \cos(\theta)$ .

### Part Rolling

We can reorient the component in plane by controlling  $x_1$  and  $y_2$ . As seen in Figure 3, the passive compliance of the gripper finger ensures that the part remains grasped. In the experiment, we controlled the voltages to Arm1 and Arm2, and measured the strain gauge outputs. The piezo drive voltages for the two arms are  $V_1 = V \sin(\alpha)$  and  $V_2 = V \cos(\alpha)$  where  $\alpha$  is the desired part orientation. We rolled a solder-coated silicon component of  $200 \mu\text{m} \times 100 \mu\text{m} \times 75 \mu\text{m}$  in the air as shown in Figure 4. In a set of initial experiments with rotation at  $10 \text{ Hz}$ , and grasping the  $75 \mu\text{m}$  by  $100 \mu\text{m}$  face, the part was rolled  $\pm 45^\circ$  successfully in 42

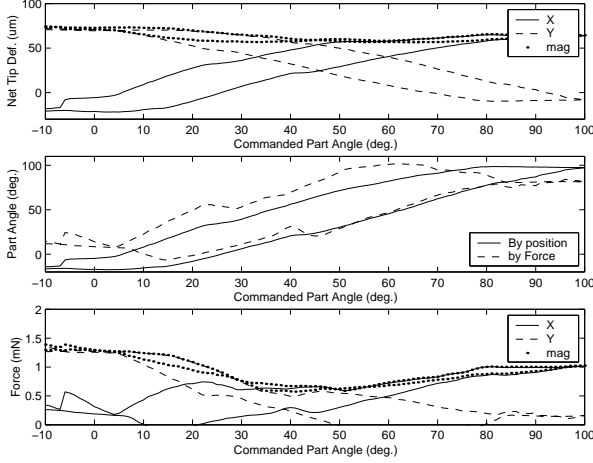


**Figure 5: Part rolling of  $200\mu\text{m} \times 100\mu\text{m} \times 75\mu\text{m}$  component. Top: net tip deflection. Middle: estimated part orientation. Bottom: sensed  $F_{1X}$  and  $F_{2Y}$  force components and sensed force magnitude.**

out of 50 trials of 100 rotations. In the 8 trials with failures, the part rotated an average of 46 (min. 12) cycles before falling out of the grip. The most likely cause of failure is the part “walking” in the grasp due to asymmetries in surface friction.

The part angle estimated from arm position measurements is  $\hat{\theta}_p = \tan^{-1} x_1/y_2$ , where  $x_1$  and  $y_2$  are calculated from the measured strains at the base and tip sheets. The estimated part angle from arm force measurements is  $\hat{\theta}_f = \tan^{-1} F_{1X}/F_{2Y}$ , where  $F_{1X}$  and  $F_{2Y}$  are calculated from the measured strains at the tips. The normalized grasping force is  $\sqrt{F_{1X}^2 + F_{2Y}^2}$ , which is kept about 1mN through all the angles. As seen in Figure 5, the estimated angles  $\hat{\theta}_p$  and  $\hat{\theta}_f$  change from 0 to  $90^\circ$  according to the commanded angle  $\alpha$ . The hysteresis on the rotation angle is jointly caused by the hysteresis of the piezoelectric actuators and the Coulomb friction deadband at the contacts. With 1 mN gripping force and assuming a largest tweezer contact area of about  $20\mu\text{m}^2$ , the contact stresses would be significantly greater than  $10^6 \text{Nm}^{-2}$ , thus dominating any dry adhesive forces [Fearing 1995].

### Pick and Place

We conducted a basic experiment to confirm that the tweezers can reliably pick and place a part. The part is placed in a dent of  $400\mu\text{m}(\text{D}) \times 200\mu\text{m}(\text{W}) \times 30\mu\text{m}(\text{H})$  to remain within the finger workspace.  $\alpha$  is kept at  $45^\circ$  and  $V$  is decreased for grasping and increased for releasing. After each grasp, the substrate stage is lowered by  $120\mu\text{m}$  in order to check whether the part is grasped in the air, then raised to the original position. It took 1.24 sec to grasp(0.16s), up-and-down(0.92s) and release(0.16s) the part. The tweezers grasped the  $75\mu\text{m} \times 100\mu\text{m}$  part face with about 1mN. There were no failures in 1000 cycles of pick and place.

### Pivot Grasp

We can also reorient a part perpendicular to the grasping plane by adding a torque through contact with a fixed “finger”, a wall attached to the substrate (Figure 6). First, the tweezers

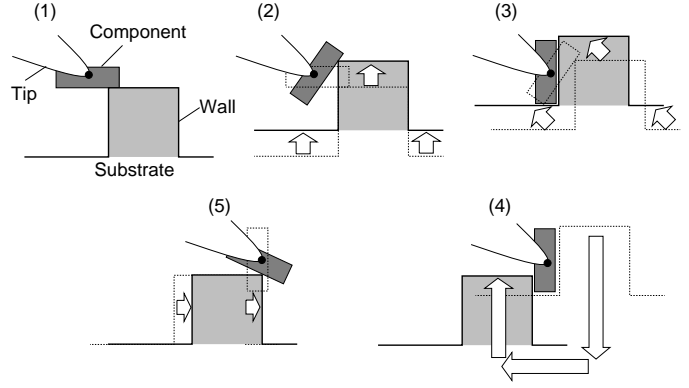


**Figure 6: “Pivot” grasp using fixture to generate moment.**

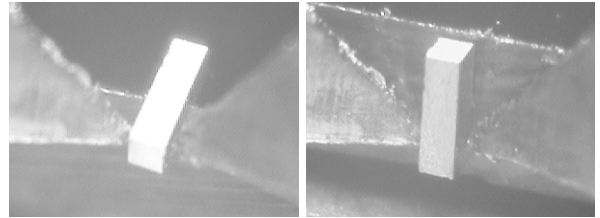


**Figure 7: “Pivot” grasp using fixture to generate moment.**

grip the part and the substrate stage is positioned such that the part is over the wall. As the stage is lifted, the edge of the wall applies a torque about the contact line between the two fingers, pivoting the part (Figure7). As described in Gopalswamy and Fearing [1989], if the friction coefficients are the same at both fingers, and the sides are parallel, for a point contact the rotation will be about a fixed axis. After being tilted, the part is pushed against the wall and made perpendicular to the substrate. Then, the wall pushes the opposite edge of the part horizontally and pivots the part to the direction parallel to the top side of the wall. In the cycle (12sec.), the part pivots  $180^\circ$ . The tweezers grasped the  $75\mu\text{m} \times 100\mu\text{m}$  face at about 1.5mN. There were no failures in 1000 cycles of  $180^\circ$ -pivot.

### Regrasp

Unlike macro parts, a submillimeter-sized part strongly sticks to other objects such as tips of manipulators. In device assembly, it is often necessary to regrasp a part for further operations such as rotation, pivot, bonding and alignment. It is possible to hold a part by vacuum, gel or another tweezer for regrasping. But it is easier to hold it without any extra devices and delicate control. We developed a “regrasping” method in which we rotated a part more than  $360^\circ$  by repeating  $90^\circ$ -rotation. As shown in Figure 8, the part grasped by the tweezers at  $\alpha = 90^\circ$  is pushed against an L-shaped wall fixed on the substrate. While the stage and Arm1 are controlled so that the wall and Arm1 keep gripping the part, Arm2 is moved to another side of the part. Next, Arm1 is moved to another side as the wall and Arm2 grip the part. Then the wall is moved away from the part and it becomes possible to rotate the part by another  $90^\circ$ . One cycle (10sec.) of  $90^\circ$  rotation of a solder-coated silicon block of  $420\mu\text{m}(\text{D}) \times 420\mu\text{m}(\text{W}) \times 100\mu\text{m}(\text{H})$  is shown in Figure 9.

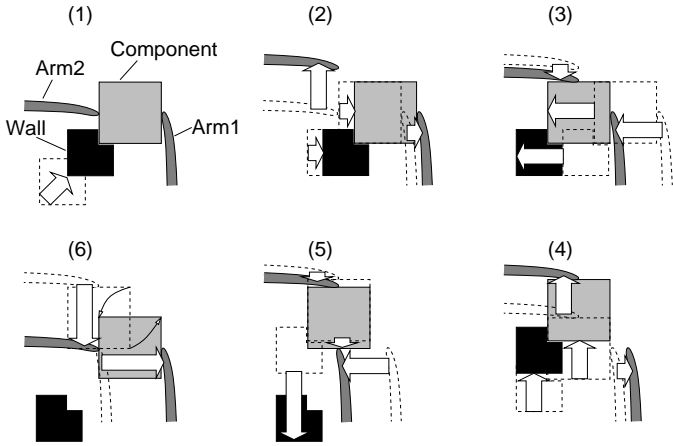


Figure 8: Regrasp using a fixed L-shaped wall

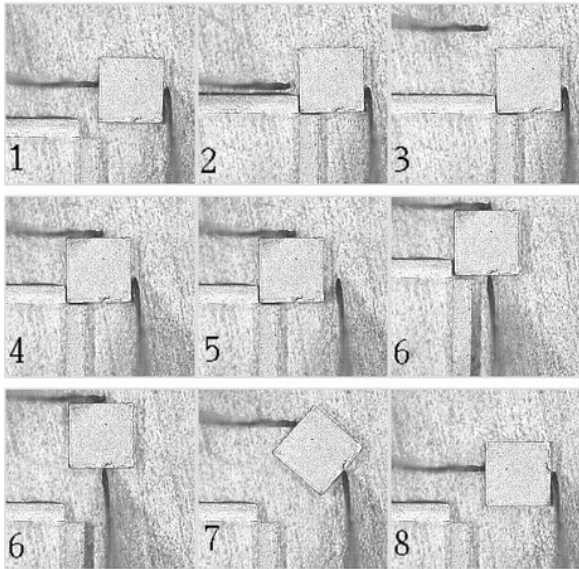


Figure 9: Regrasp using a fixed L-shaped wall

There were only 2 failures in 5000 cycles of regrasping and 90°-rotation. In the two failures, the part translated in the gripper above the edge of the wall. The wall is  $125\mu\text{m}(\text{W}) \times 100\mu\text{m}(\text{H})$ .

### Alignment

Due to the lack of reliable force information, it is difficult to align a sub-millimeter part through video microscopes. Thus, we might break parts by applying too large forces or misalign them because of insufficient force. Consider aligning a part along a plain wall, using two tweezers. (Zesch and Fearing [1998] used a single force sensing probe). We simply grasped and pushed a part toward a wall (Figure 10). After the part reached the wall, it slid and rotated between two arms due to geometrical constraints and finally approximately aligned itself with the wall.

Although the pushing force can not be measured directly, the grasping force limits the maximum friction force between the fingers and the part. Therefore the maximum of pushing

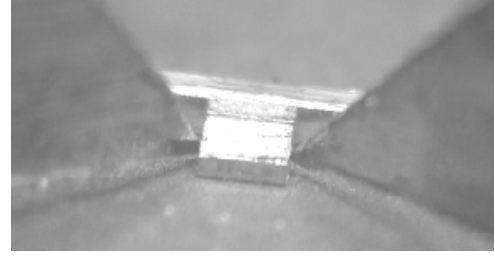


Figure 10: Pushing for alignment

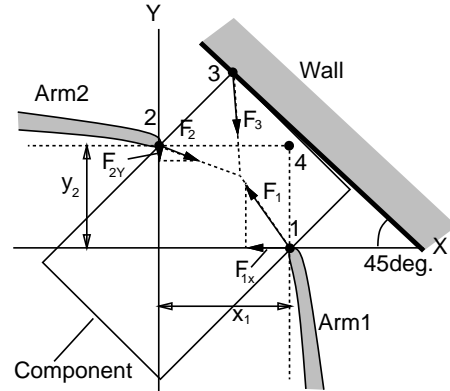


Figure 11: Alignment check method

force can be controlled by the grasping force. (We ignore the friction between the part and the substrate, because the grasping force ( $\approx 3\text{mN}$ ) is far bigger than the gravity force ( $\approx 400\text{nN}$ ) on the part.) In order to detect part alignment, we measured the moment around Point4 when we sent a  $\pm 15^\circ$  rotation command (Figure 11). We define the moments around Point4 by Arm1, Arm2 and the wall as  $M_1$ ,  $M_2$  and  $M_w$  respectively. In the static situation,  $M_1 + M_2 + M_w = 0$ . Therefore  $M_w = -(M_1 + M_2) = F_{1x}y_2 - F_{2y}x_1$ . If the part isn't touching the wall,  $M_w$  should be 0. In fact,  $M_w$  was  $\approx 0$  when the part isn't touching the wall (Figure 12).  $M_w$  changes in positive and negative range according to the commanded part angle, when the part is well aligned. Otherwise, it means that the part is well aligned. The hysteresis of  $M_w$  is caused by the hysteresis of the piezoelectric actuators. (The part is a solder-coated silicon block of  $420\mu\text{m}(\text{D}) \times 420\mu\text{m}(\text{W}) \times 100\mu\text{m}(\text{H})$ .)

### Demonstration Structure

By combining the “part rolling”, “pivot grasp”, and “re-grasping” methods, it is possible to control the orientation of part freely. In order to demonstrate the usefulness of these dextrous micromanipulation techniques, we made a sample structure by manually attaching 4 micro-components with a UV-curing adhesive, Loctite 352 as in Figure 13b. The size of the three base components is  $75 \times 230 \times 400\mu\text{m}$ , and the top small component is  $80 \times 80 \times 430\mu\text{m}$ . Parts started out flat on the substrate, and we used the dextrous manipulation techniques mentioned above to reorient each component three-dimensionally. The adhesive

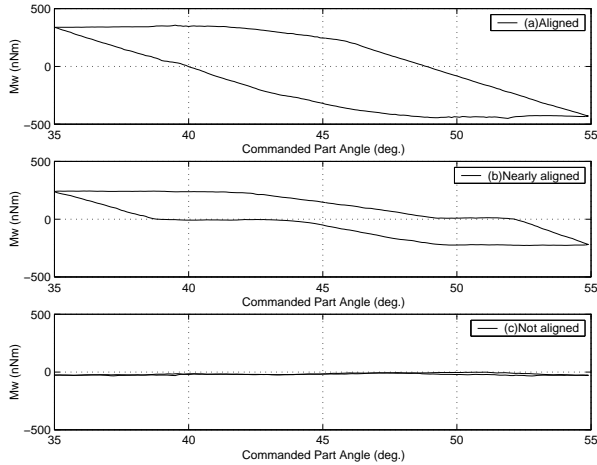


Figure 12: Moment by the wall

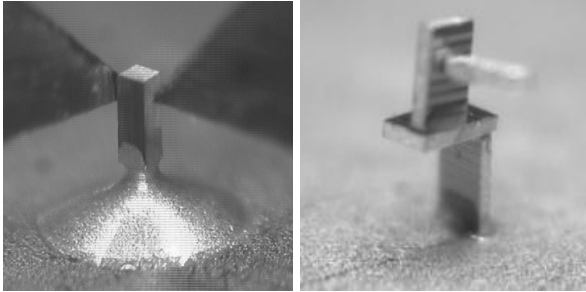


Figure 13: a) Adhesive applied to micropart. b) Stacked microparts.

was applied by dipping one edge of each component into the adhesive drop on the substrate as seen in Figure 13a. UV light was applied to cure the adhesive for 3 minutes while each component was held on the structure by the tweezers.

### CUTTING AND FOLDING OF MICROSTRUCTURES

As a technique for building microstructures with high strength-to-weight ratio and low-friction flexural joints we have developed a process using laser cutting of thin sheet metal followed by folding. We use a New Wave Quiklaze laser micromachining station which consists of a laser, focussing microscope, and a Prior XYZ microstepping stage. The microstepping stage has submicron resolution. The laser has a wavelength of 532 nm (green) and delivers 0.6 mJ per pulse with a maximum rate of 40 Hz. Typically, we focus down to a square spot  $50\ \mu\text{m}$  wide. At this spot size, cutting through  $13\ \mu\text{m}$  thick stainless steel requires about 1 second (40 pulses).

Although the laser can be focussed down to  $2\ \mu\text{m}$ , we find that it is difficult to cut a line much thinner than the thickness of the metal. For  $13\ \mu\text{m}$  thick metal, we successfully cut a  $10\ \mu\text{m}$  line. Below this, the metal does not cleanly separate. There are two possible reasons for this. First, since the laser has a very large angle of focus, the top of the trench may block the beam at the bottom of the trench. Second, for each pulse of energy, the metal does not completely vaporize and disappear. Rather,

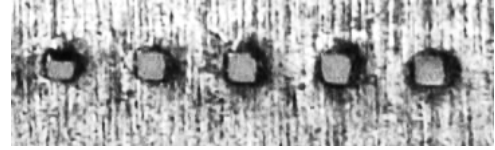


Figure 14: Laser cut fold line with 50% cut pattern. Cuts are  $50\ \text{by}\ 50\ \mu\text{m}$ .

some of it is molten and “splatters”. With a very thin trench, there is not an escape route for this material and it tends to hit the side of the trench, filling in behind the laser as it moves along.

We desire our cutting and scoring process to be robust against errors so we have designed the algorithms to not rely on precise timing between the controlling computer and the XYZ stage, nor on precise power output from the laser.

The usual approach to make a fold line is to create a continuous line which cuts partially into the surface of the metal. To accomplish this in laser micromachining would require reducing the laser power and precisely timing its motion over the surface so that it cuts into the metal but not all the way through. Since this is error-prone, we instead use an algorithm which creates a “dotted line”, cutting a single punch hole of the laser beam diameter at intervals along the score line, about one hole every three beam diameters (Figure 14). A disadvantage of this method is that more stress may be created around the punch hole, weakening the metal as it is folded.

The usual approach for cutting a line through sheet metal is to move the piece at a continuous slow feed rate so that the laser has enough time to cut through the metal. This has two problems. First, we have had trouble finding a microstepping controller which could be configured with such a slow feed rate. ( $13\ \mu\text{m}$  thick sheet metal would need less than  $50\ \mu\text{m}$  per second at our laser power.) Second, this creates problems with the stop and end points of a line since we would need extra wait times to make sure the laser cuts fully through. Instead, we use an algorithm which is more like a “nibbler” tool. The beam cuts completely through the metal and then the XYZ stage moves over half a beam diameter where the laser cuts completely through again, and so on. As with the scoring algorithm, this has the advantage of a “binary” depth. Also, we do not rely on precise calibration of a feed rate in the microstepping controller since it moves in discrete steps.

In cutting and scoring we also take advantage of the stage controller’s built-in autofocus. At configurable intervals along the cut or score line, the algorithm turns off the laser, moves the stage slightly off the line so that the camera has a clear image of the sheet metal surface, autofocuses, repositions and resumes. This keeps the laser in focus over variations in the sheet metal height.

### Bending Analysis

To accurately fold sheet metal, knowledge of the required bending moments [Hill 1950] and of the amount of springback in the metal is useful in the design of the bending fixtures. The analysis by Leu [1997] will be used here to estimate these values. Consider the section to be folded, of length  $l$  and width  $w$ , as

in Figure 15. The desired bending force is a pure moment,  $M$ ,

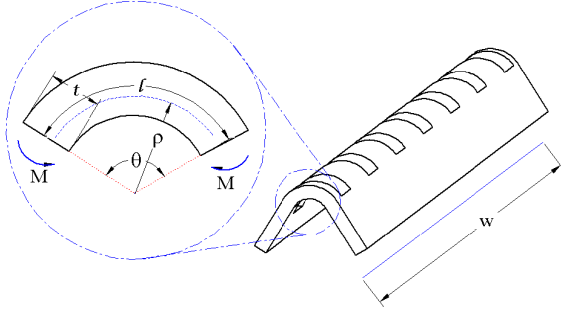


**Figure 15: Sheet metal folding**

because this gives a uniform curvature throughout the section. Although a pure moment is difficult to achieve, forces can be made negligible with a suitable bending fixture. When the radius of curvature of the bend,  $\rho$  (as measured from the neutral axis, the section which doesn't experience any transverse strain), is on the same order of magnitude as the sheet thickness,  $t$ , the radial compressive forces cannot be ignored as is assumed in many bending calculations and a large fraction of the metal is operating in its plastic range. Under the assumption of plane strain,  $M$  is given by:

$$M = \frac{\eta w S_Y e^n t^{n+2}}{2^{n+2} \rho^n (1+n)n^n} \left( \frac{1+R}{\sqrt{1+2R}} \right)^{1+n} \quad (1)$$

where  $\eta$  is a scale factor to account for the scoring scheme described in the previous section (*e.g.*, when only every third spot is blasted, then  $\eta = 2/3$ ),  $S_Y$  is the yield strength,  $R$  is the normal anisotropic value and  $n$  is the strain hardening exponent. The resulting springback angle fraction after unloading is given by:

$$\frac{\Delta\theta}{\theta} = \frac{3S_Y e^n (1-\nu^2)}{2E(1+n)n^n} \left( \frac{1+R}{\sqrt{1+2R}} \right)^{1+n} \left( \frac{t}{2\rho} \right)^{n-1} \quad (2)$$

where  $E$  is the Young's modulus,  $\nu$  is the Poisson ratio, and  $\theta$  is the angle before unloading ( $\rho\theta = l$ ).

It is interesting to note that in the case of no work hardening ( $n = 0$ ) equations (1) and (2) show that, in the plastic range, the required bending moment and the springback angle do not depend on the amount of bending (*i.e.*, on  $\theta$  or  $\rho$ ). In actuality, for most steels,  $0.1 < n < 0.3$ . The anisotropic value may be significant, especially in sheet metals which are typically cold-rolled. The axis of bending should be chosen perpendicular to the direction of rolling when possible.

#### **Example Structure: MFI Thorax**

As an example, consider the folding for the thorax structure in the micromechanical flying insect (MFI) described by Fearing et al [2000] (Figure 17b). The material used here is stainless steel 302 which has  $S_Y = 520\text{MPa}$ ,  $E = 190\text{GPa}$ , and  $\nu = 0.30$ . The plate thickness is  $t = 12.5\mu\text{m}$  and the effective width to be folded (including all the links) is  $w = 20\text{mm}$ . The length over which the bending takes place is the laser spotsize,  $l = 50\mu\text{m}$ , and the desired final angle is  $\theta = 120^\circ = \frac{2\pi}{3}\text{rad}$ . Unfortunately, values

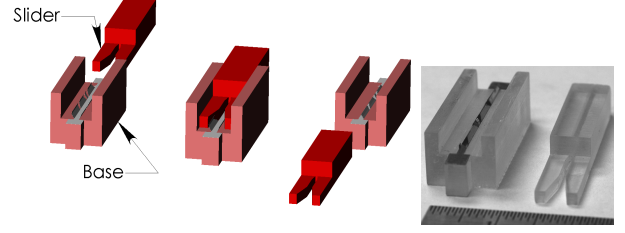


**Figure 16: Folding with fixtures.**

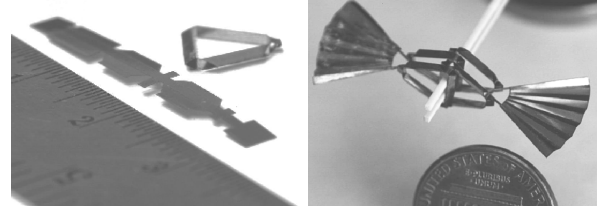


**Figure 17: a) Unfolded and folded flexural 4 bar mechanism. b) Thorax and wing structure for flying micro-robot.**

for  $n$  and  $R$  are often not readily available and here, they are taken simply as  $n = 0.2$  and  $R = 1$  (*i.e.*, isotropic). Substituting these values into equations (1) and (2) results in  $M = 0.35\text{N}\cdot\text{mm}$  and  $\Delta\theta = 0.018\text{rad} = 1.0^\circ$ .

A simple folding fixture is shown in Figure 16. The steel part is manually pre-bent in order to encourage bending at the score lines and to form edges on which the fixtures can apply forces. The pre-bent piece is attached to the base fixture while a sliding fixture is swept over it. The underside of the slider narrows into the desired final shape, which in this case is an equilateral triangle. The problem of springback here is avoided by applying an adhesive to the folded structure from behind the slider as it moves along. The fixtures shown were fabricated on a stereolithography apparatus (3D Systems SLA250-HR). The cyanoacrylate adhesives used do not adhere well to the cured photopolymer from which the fixtures are made, thus it is easy to remove the assembled structure from them.

The laser-cut stainless steel piece which is part of the thorax for the construction of the MFI, is shown in Figure 17a. Tabs at the end of the piece permit the part to be attached to a folding fixture and these sacrificial tabs are broken off easily after the folding is completed.

The pre-bending operation is done under a microscope by applying a line force on the scored edge to be bent, sliding a razor blade under one side of the edge and then rotating the blade about the edge so that a fairly uniform moment is applied. Initial attempts to automate this task have not achieved the same quality of bending as this manual method, primarily because of the tight tolerances needed. These tolerances may be loosened, for example, by a higher frequency of score marks or by accurately controlling the depth of the cut in the desired bend section. Both examples rely on reducing the area moment of inertia in the section, making it easier to bend; the latter method has the advantage that less cutting is necessary for the same effective reduction but accurate depth control is difficult

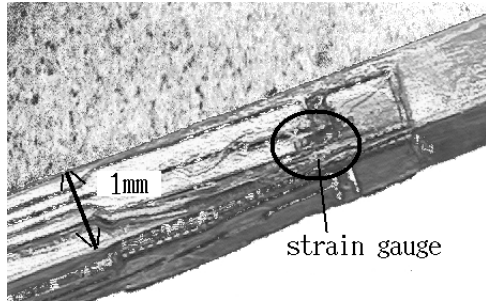


**Figure 18: Folded flex circuit with strain gauge mounted on 1 mm box beam.**

with our setup.

Some sensors and actuators may be more easily added onto the planar structure before folding while others may be easier to add afterwards (*e.g.*, in some designs, the folding would be difficult to perform if the actuator is attached first). As an example, Figure 18 shows a laser-cut flex circuit mounted on a 1 mm box beam. The 1 mm  $\times$  0.15 mm strain gauge is attached to the flex circuit before the circuit is wrapped around the beam.

#### FUTURE WORK IN AUTOMATED FOLDING

Conceptually, fully automated assembly of folding structures is possible. Figure 19b shows an overview of the combined cutting/folding apparatus. A block is mounted on the XYZ stage which holds the sheet metal during laser cutting and has the pressing mold which is used to fold the sheet metal, as well as a small reservoir for glue. Suspended above the platform (from left to right) are the laser, the folding press, two clips for folding and holding the part, and a glue dipping stick.

The sheet metal is initially fastened to the face of the block above the folding mold. The XYZ stage positions and moves the sheet metal (and mold) beneath the laser which scores the fold lines and cuts the outer circumference of the piece. A few small tabs remain in the cutout so that the part does not fully release until the folding press pushes it into the mold. After cutting, the XYZ stage pushes the piece up under the folding press which pushes the sheet metal into the mold, similar to cardboard box folding. Next the clips are used to create the final fold and hold the piece in place while the XYZ stage moves to the gluing stick. The stick is first placed in the glue reservoir and then on the piece to secure the fold.

It is possible to use laser-micromachining to build simple thermal actuators, to reduce the need to attach and wire other actuators to the structures. Figure 19a shows a possible design for a thermal actuated finger which could be used for the micropart manipulation discussed in the micro-assembly section. The thermal actuator can be constructed from a heated thin beam mechanically coupled to an unheated thick beam [Lerch et al 1996]. The two beams are electrically in series. When a voltage is applied across the beams, current flows which heats up the “thin” beam more than the “thick” beam causing the actuator to bend. Note that most of the voltage drop occurs over the “thin” beam, thus if the end of the thick beam is grounded, the tip of the arm which touches objects will also be near ground. For a 200  $\mu\text{m}$  thermal actuator beam with coefficient of thermal

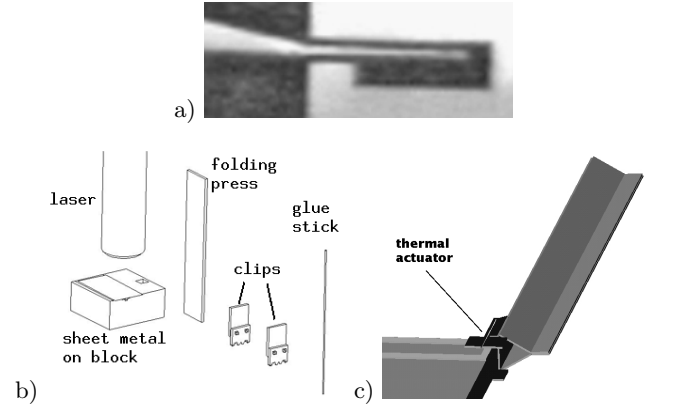


**Figure 19: a) Heatuator cut from stainless steel (beams are dark). b) Fixtures for automatic folding of triangular beam. c) Plan for thermally actuated finger.**

expansion  $17 \times 10^{-6}/^{\circ}\text{C}$ , heating by  $200^{\circ}\text{C}$  will bend the actuator by 0.034 radians, and displace a 3 mm long arm 100  $\mu\text{m}$  at the tip. This is sufficient to manipulate small parts.

#### CONCLUSION

We made dextrous tweezers which consist of two 1 DOF compliant fingers perpendicular to each other. Strain gauges were used to monitor the deflections, forces and part rolling angle. We have shown that the tweezers can be dextrous and robust in manipulation of submillimeter-sized parts, even without closing a sensing loop. The tweezers by themselves can pick-and-place and roll parts. With help of a few fixtures on a 3 DOF cartesian stage, the tweezers can reliably pivot and regrasp the part by continually applying contact forces which greatly exceed micro-scale adhesion forces. By measuring contact generated moments on the part through strain gauges, we can tell whether the part is aligned with a wall. For the demonstration of these techniques, a structure was made by bonding 4 micro-parts using UV-glue. With appropriate part pallets, this assembly process could be automated. By arranging a bunch of miniaturized dextrous tweezers, it could also be possible to operate parallel assembly with only one XYZ cartesian stage.

A cutting and folding process based on laser micromachining of 12  $\mu\text{m}$  thick stainless has been developed. Using a line of holes for bend lines, stainless steel can be plastically deformed to make hollow beam structures such as 4 bar mechanisms. Simple fixtures ease the folding and handling of 1 mm beams. Circuitry and sensors can be attached using flex circuit board bonded to the structure.

We have discussed two complementary processes for prototyping microstructures which could be used together to fabricate micro-robots. In the first process, dextrous micromanipulation and adhesive bonding or soldering could be used to build rigid structures and attach electronic components. In the second process, lightweight, high-strength structures with flexural joints can be cut from thin sheet metal and folded to the final shape. We plan that complete microrobots, such as a micromechanical flying insect, could be made by the combination of folded structures with micro-assembled electronics, actuators and sensors.

## ACKNOWLEDGMENTS

The authors thank Chris Keller and MEMS Precision Instruments for providing microparts and helpful discussions, and Wolfgang Zesch for developing the first version of the micromanipulation system.

## REFERENCES

- [1] F. Arai, D. Ando, T. Fukuda, T. Nonoda, and T. Oota, "Micro Manipulation Based on Micro Physics-strategy based on attractive force reduction and stress measurement", (*Proc. IEEE/RSJ Intelligent Robots and Systems*, pp. 236-241, Pittsburgh, PA, August 3-5, 1995.
- [2] F. Arai and T. Fukuda, "Adhesion-type Micro Endeffector for Micromanipulation" *IEEE Int. Conf. Robotics and Automation*, Albuquerque, New Mexico, April 1997.
- [3] R. C. Brost, "Automatic Grasp Planning in the Presence of Uncertainty", *IEEE Int. Conf. on Robotics and Automation*, San Francisco, CA, April 1986.
- [4] B. Carlisle, K. Goldberg, A. Rao, and J. Wiegley. "A pivoting gripper for feeding industrial parts," *IEEE Int. Conf. on Robotics and Automation*, San Diego, May 1994.
- [5] A. Codourey, W. Zesch, R. Buechi, and R. Siegwart, "A Robot System for Automated Handling in Micro-World", *Proc. IEEE/RSJ Intelligent Robots and Systems*, pp. 185-190, Pittsburgh, PA, August 3-5, 1995.
- [6] M.B. Cohn, K.F. Bohringer, J.M. Noworolski, A. Singh, C.G. Keller, K.Y. Goldberg, and R.T. Howe, "Microassembly Technologies for MEMS," *SPIE Micromachining and Microfabrication*, Santa Clara, CA Sept. 1998.
- [7] M. Erdmann, M. T. Mason, and G. Vanecek Jr. "Mechanical parts orienting: The case of a polyhedron on a table," *Algorithmica*, vol. 10, no. 2, Special Issue on Computational Robotics. August 1993.
- [8] R.S. Fearing "Implementing a Force Strategy for Object Re-orientation," *IEEE Int. Conf. on Robotics and Automation*, San Francisco, CA April, 1986a.
- [9] R.S. Fearing, "Simplified Grasping and Manipulation with Dexterous Robot Hands", *IEEE Journal of Robotics and Automation* Vol RA-2, No.4, December 1986b.
- [10] R.S. Fearing, "Survey of Sticking Effects for Micro-Parts", *IEEE Int. Conf. Robotics and Intelligent Systems IROS '95*, Pittsburgh, PA August 7-9, 1995.
- [11] R.S. Fearing, K.H. Chiang, M. Dickinson, D.L. Pick, M. Sitti, and J. Yan, "Wing Transmission for a Micromechanical Flying Insect", to appear *IEEE Int. Conf. on Robotics and Automation*, San Francisco, CA April 2000.
- [12] J.T. Feddema and R.W. Simon, " Visual servoing and CAD-driven microassembly," *IEEE Robotics and Automation Magazine*, Dec. 1998, vol.5, (no.4):18-24.
- [13] J.T. Feddema and T.R. Christensen, "Parallel Assembly of LIGA Components", Tutorial on Modelling and Control of Micro and Nano Manipulation, *IEEE Int. Conf. on Robotics and Automation*, Detroit, Mich, May 1999.
- [14] K. Goldberg, "Orienting Polygonal Parts Without Sensors", *Algorithmica, Special Issue on Computational Robotics*, vol. 10, no. 3, pp. 201-225, August, 1993.
- [15] S. Gopalswamy and R.S. Fearing, "Grasping of Polyhedral Objects with Slip", *IEEE Int. Conf. on Robotics and Automation*, Scottsdale AZ, May 1989.
- [16] R. Hill, *The Mathematical Theory of Plasticity*, Glasgow: Oxford University Press, 1950.
- [17] E.E. Hui, R.T. Howe, and M.S. Rodgers, "Single-Step Assembly of Complex 3D Microstructures," MEMS 2000, Japan.
- [18] T. Kasaya, H. Miyazaki, S. Saito, and T. Sato, "Micro Object Handling under SEM by Vision-based Automatic Control", *SPIE Conf. on Microrobotics and Micromanipulation*, vol. 3519, pp. 181-188, Boston, MA Nov. 1998.
- [19] P. Lerch, et al, "Modelization and Characterization of Asymmetrical Thermal Micro-actuators", *Journal of Micromechanics and Micro-engineering*, No. 6, pp. 134-137, 1996.
- [20] D.-K. Leu, "A Simplified Approach for Evaluating Bendability and Springback in Plastic Bending of Anisotropic Sheet Metals," *Jnl. of Materials Processing Technology*, vol. 66, pp. 9-17, 1999.
- [21] L. Lu and S. Akella, "Folding Cartons with Fixtures: A Motion Planning Approach", *IEEE Int. Conf. Robotics and Automation*, pp. 1570-1576, Detroit, MI, May 1999.
- [22] K. Lynch, "Toppling Manipulation," *IEEE Int. Conf. Robotics and Automation*, pp. 2551-2557, Detroit MI, May 1999.
- [23] B.J. Nelson, Y. Zhou, and B. Vikramaditya, "Sensor-Based Microassembly of Hybrid MEMS Devices", *IEEE Control Systems*, pp. 35-45, Dec. 1998.
- [24] K.S.J. Pister, M.W. Judy, S.R. Burgett, and R.S. Fearing, "Micro-fabricated Hinges", *Sensors and Actuators A*, vol. 33, pp. 249-256, 1992.
- [25] A. Rao, D. Kriegman, and K. Goldberg, "Complete algorithms for feeding polyhedral parts using pivot grasps," *IEEE Transactions on Robotics and Automation*, vol. 12, no. 6, April 1996.
- [26] D. Rus, "Coordinated Manipulation of Polygonal Objects" *IEEE/RSJ Int. Conf. on Intelligent Robots and Systems*, pp. 106-112, Yokohama, Japan, July 26-30, 1993.
- [27] S. Saito, H. Miyazaki, and T. Sato, "Pick and Place Operation of a Micro Object with High Reliability and Precision based on Micro-Physics under SEM", *IEEE Int. Conf. Robotics and Automation*, pp. 2736-2743, Detroit MI, May 1999.
- [28] I. Shimoyama, H. Miura, K. Suzuki, Y. Ezura, "Insect-Like Micro-robots with External Skeletons", *IEEE Control Systems Magazine*, pp. 37-41, 1993.
- [29] M. Sitti and H. Hashimoto, "Two-Dimensional Fine Particle Positioning Using a Piezoresistive Cantilever as a Micro/Nano-Manipulator", *IEEE Int. Conf. Robotics and Automation*, pp. 2729-2735, Detroit MI, May 1999.
- [30] A. Sulzmann, P. Boillat, and J. Jacot, "New Developments in 3D Computer Vision for Microassembly", *SPIE Conf. on Microrobotics and Micromanipulation*, SPIE vol 3519, pp. 36-42, Boston, MA Nov. 1998.
- [31] J. Wiegley, K. Goldberg, M. Peshkin, and M. Brokowski, "A complete algorithm for designing passive fences to orient parts," *Assembly Automation*, vol. 17, no. 2, August 1997.
- [32] R. Yeh, E.J. Kruglick, M. Klitzke, and K.S.J. Pister, "Towards an Articulated Silicon Microrobot" *Winter Annual Meeting, ASME*, Dec. 1994.
- [33] T. Yoshikawa, Y. Yokokohji, and A. Nagayama, "Object Handling by 3 finger hands using slip motion" *IEEE/RSJ Int. Conf. on Intelligent Robots and Systems*, pp. 99-105, Yokohama, Japan July 26-30, 1993.
- [34] W. Zesch and R.S. Fearing, "Alignment of Microparts Using Force Controlled Pushing," *SPIE Conf. on Microrobotics and Micromanipulation*, Nov. 2-5 1998, Boston, MA, USA.
- [35] W. Zesch, M. Brunner, and A. Weber. "Vacuum Tool for Handling of Micro-objects in a Nanoenvironment," *Proc. IEEE Int. Conf. Robotics and Automation*, pp. 1761-1766, Albuquerque, NM April 1997.
- [36] Y. Zhou and B.J. Nelson, "Adhesion force modeling and measurement for micromanipulation", *SPIE Conf. on Microrobotics and Micromanipulation*, vol. 3519, pp. 169-180, Boston, MA, Nov. 1998.